RESEARCH ARTICLE   **OPEN ACCESS**

IMPACT OF NITROGEN INCORPORATION ON BAND GAP BOWING IN ZINC-BLENDE GAAS$_{1-x}$N$_x$: A FIRST-PRINCIPLES STUDY

Mimouna Oukli [1], Ghlam Karima[2], Seyfeddine Bechekir[3]

[1,3]Applied Materials Laboratory (A.M.L), Faculty of Electrical Engineering, Djillali Liabes University of Sidi Bel Abbes, Sidi Bel Abbes, Algeria.
[2]Laboratory of Intelligent control And Electrical Power System (ICEPS), Djillali Liabes University of Sidi Bel-Abbès, Sidi Bel-Abbès, Algeria

[1]http://orcid.org/0000-0002-4871-6919 , [2]http://orcid.org/0000-0001-8276-0609 , [3]https://orcid.org/0000-0002-6143-7164

Email: mounaoukli@yahoo.fr, ouklimouna22@gamil.com, Karighlam16@yahoo.fr,

ARTICLE INFO	ABSTRACT
	This study, utilizing full-potential linear muffin-tin orbital (FPLMTO) calculations within density functional theory (DFT), delved into the structural properties of zinc-blende GaAs$_{1-x}$N$_x$ alloys. By varying the nitrogen concentration (x= (0.125, 0.083, and 0.063), we observed deviations from Vegard's law for lattice parameters and nonlinear behavior of the bulk modulus. The band gap bowing was primarily attributed to volume deformation effects, as elucidated by the Ferhat approach. Our findings demonstrate that the electronic and structural properties of GaAs$_{1-x}$N$_x$ are strongly influenced by the nitrogen concentration. These variations present exciting opportunities for bandgap engineering and the design of wide-bandgap optoelectronic devices.

I. INTRODUCTION

Dilute nitride alloys, such as GaAs$_{1-x}$N$_x$ and GaSb$_{1-x}$N$_x$, have emerged as promising materials for infrared optoelectronic devices, particularly for telecommunications applications including solar cells [1], long-wavelength light-emitters (1.3 μm–1.55 μm), and tunable photodetectors [2-8]. These alloys offer unique properties, notably a significant reduction in their bandgap energy, rendering them highly attractive for various applications [9-10]. This band gap reduction is primarily attributed to the incorporation of a small amount of nitrogen [11] (typically less than 5%) into III-V compounds [12-14]. This phenomenon, known as "bowing," is linked to the strong curvature of the relationship between alloy composition and bandgap energy that has been experimentally observed for some dilute nitrides such as GaPN [15], [16], InPN [17] and GaAsN [18]. The "bowing factor," a key characteristic of these materials, is influenced by factors such as the electronegativity and atomic radius of nitrogen compared to those of arsenic [19].

While the band gap of a typical mixed compound exhibits a linear relationship with composition, as described by Vegard's law, certain materials, like GaNAs, GaInNAs, and GaNP, deviate significantly from this behavior, exhibiting a large band gap bowing with a bowing coefficient as large as 20 eV [20]. This

anomalous decrease in band gap, often termed "large band gap bowing," has been extensively studied using theoretical and computational methods [21-32]. To gain a deeper understanding of the factors influencing this bowing effect, theoretical and computational methods have been extensively employed. However, the underlying mechanisms remain elusive.

To explore the underlying causes of this bowing phenomenon, measurements and calculations on semiconductor alloys indicate that the band gap energy deviates from the linear behavior given by Vegard's law [33], termed 'large band gap bowing'. The magnitude of the bowing factor varies significantly among different alloys and its physical origins are not fully understood. Our phenomenological model aims to elucidate these factors by investigating the structural properties of III-V ternary alloys containing nitrogen in zinc blend structure. To better understand the physical origins of the large dispersion and composition-dependent bowing in A$_{1-x}$B$_x$C alloys, we have used our recently developed phenomenological model Ferhat [34], which has been shown to account successfully for the optical band gap bowing of III–V semiconductor alloys.

This study investigates the impact of nitrogen incorporation on the gap bowing behavior of zinc-blende GaAs$_{1-x}$N$_x$ alloys. We will further explore the influence of nitrogen incorporation on this phenomenon. Full-potential linear muffin-

tin orbital (FPLMTO) calculations within density functional theory (DFT) will be employed to systematically study these alloys over a range of compositions.

The paper is organized as follows. The method is briefly commented in Section 2. Results are discussed in Section 3. Finally, in section 4 we summarize the main conclusions of this work

II. COMPUTATIONAL DETAILS

This study employed the extended FPLMTO (PLW) method [35-37] for its calculations. This method, capable of handling all types of structures, including open ones, describes the electron exchange-correlation energy using the local density approximation (LDA) [38] and the Perdew et al. [39] parameterization. The computations were performed using the lmtART computer code [38], [40], which expands the potential within the non-overlapping muffin-tin sphere in spherical harmonics and the s, p, and d basis functions in plane waves in the interstitial regions. Convergence of the calculations was achieved when the total energy reached an accuracy of 10^{-4} Ry.

For the binary compounds under investigation, a cubic unit cell containing four atoms was considered. Each lattice site is occupied by two atoms: a gallium (Ga) atom located at the origin $(0, 0, 0)a_0$, and a nitrogen (N) or arsenic (As) atom positioned at $(1/4, 1/4, 1/4)a_0$ in the zinc blende structure (where a_0 is the lattice parameter for both binary compounds).

Tetragonal unit cells of 16, 24, and 32 atoms were used for ternary systems with x=0.125, x=0.083, and x=0.063, respectively. A primitive cell was used for binary systems.

The optical bandgap bowing (b) in a binary alloy system was analyzed by decomposing it into three contributions [34], [41]: volume deformation (VD), charge exchange (CE), and structural relaxation (SR). The VD term represents the response of binary compounds to pressure changes, the CE term relates to charge transfer at a = a(x), and the SR term describes the change in the ban dgap during relaxation.

For a given average concentration of x, the ternary alloy exhibits the following reaction:

$$(1 - x)\text{GaAs}_{(aGAS)} + x\text{GaN}_{(aGaN)} \rightarrow \text{GaAs}_{1-x}\text{N}_x(a_{eq}) \quad (1)$$

Where aGaAs and aGaN are the equilibrium lattice parameters of the parent materials GaAs and GaN, respectively, the equilibrium lattice parameter of the ternary alloy GaAs$_{1-x}$ N$_x$ varies with x.

Equation (1) can be decomposed into three steps:

$$\text{GaAs}_{(aGAS)} + \text{GaN}_{(aGaN)} \rightarrow \text{GaAs}(a) + \text{GaN}(a) \quad (2)$$

$$(1 - x)\text{GaAs}_{(aGAS)} + x\text{GaN}_{(aGaN)} \rightarrow \text{GaAs}_{1-x}\text{N}_x(a) \quad (3)$$

$$\text{GaAs}_{1-x}\text{N}_x(a) \rightarrow \text{GaAs}_{1-x}\text{N}_x(a_{eq}) \quad (4)$$
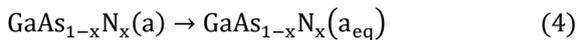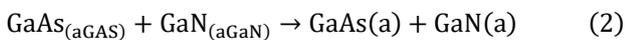
The first step quantifies the impact of volume deformation on the bowing parameter by analyzing the relative response of GaN and GaAs to hydrostatic pressure. This is followed by considering the charge transfer between GaN and GaAs, and finally, the relaxation of the alloy's bonds. The overall bowing parameter is determined by summing up these three contributions.

These terms were calculated for various concentrations (x=0.125, x=0.083, and x=0.063) to determine the total bowing

effect at the direct energy gap E $_{\Gamma\Gamma}$. The construction of total bowing is:

$$b = b_{VD} + b_{CE} + b_{SR} \quad (5)$$

Ferhat and Bechstedt proposed a model for the bandgap bowing parameter in the ternary GaAs$_{1-x}$N$_x$ alloy [42]. This model posits that the bowing parameter is composed of three distinct contributions, each dependent on the nitrogen concentration (x), which was investigated for x = 0.125, 0.083, and 0.063 in this study. These contributions are defined by specific mathematical relationships [2, 3]

$$b_{VD} = \frac{E_{GaAs}(a_{GaAs}) - E_{GaAs}(a)}{1 - x} + \frac{E_{GaN}(a_{GaN}) - E_{GaN}(a)}{x} \quad (6)$$

$$b_{CE} = \frac{E_{GaAs}(a)}{1 - x} + \frac{E_{GaN}(a)}{x} - \frac{E_{Ga1-xNx}(a_{eq})}{x.(1 - x)} \quad (7)$$

$$b_{SR} = \frac{E_{GaAs1-xNx}(a) - E_{GaAs1-xNx}(a_{eq})}{x.(1 - x)} \quad (8)$$

Where the equilibrium lattice constants of GaAs and GaN are represented by a_{GaAs} and a_{GaN} respectively, and the equilibrium lattice constant of the alloy with the average composition x is represented by *aeq*. The energy gaps of the binary compounds GaAs and GaN are represented by E_{GaAs} and E_{GaN} respectively, and the energy gap of the alloy GaAs$_{1-x}$N$_x$ for x=0.125, 0.083 and 0.063 is represented by E (GaAs$_{1-x}$N$_x$).

III. RESULTS AND DISCUSSIONS

In this section, we investigate the electronic properties of the parent binary compounds GaN and GaAs, as well as their ternary alloys, by computing their band structures using our calculated lattice parameters.

The total energy of each binary compound and the ternary GaAsN, as a function of volume, is depicted in Figures 1 through 5. These plots visualize how the total energy of the systems changes when their volume is altered.
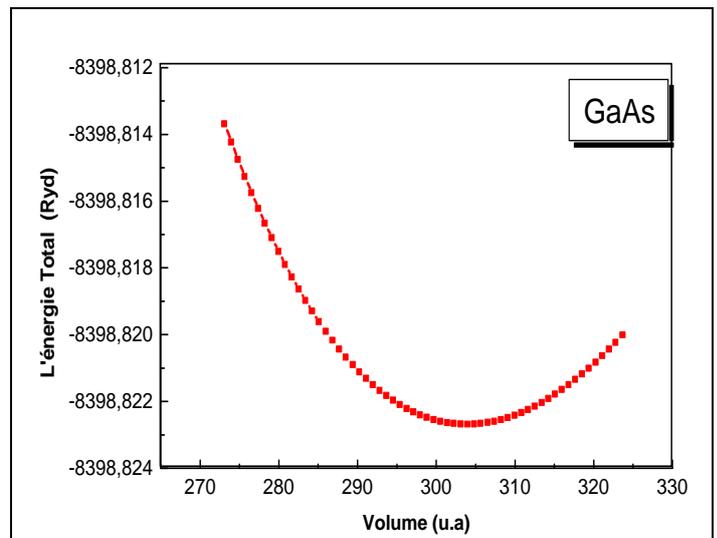
Figure 1: Total energy per molecule as a function of volume for GaAs using LDA calculation.
Source: Authors, (2024).
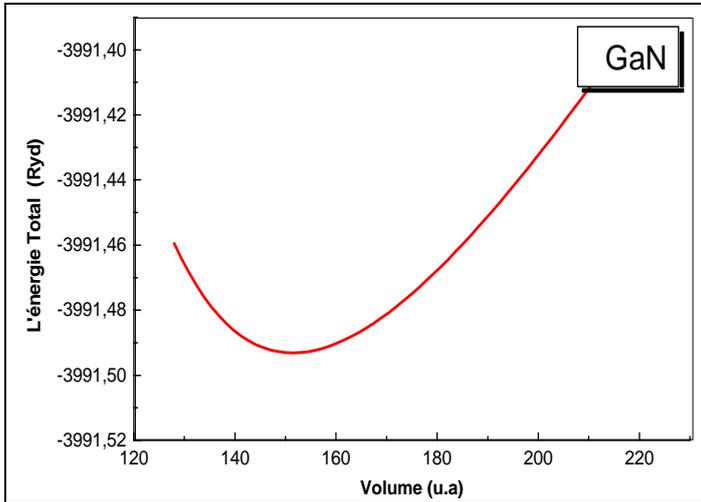
Figure 2: Total energy per molecule as a function of volume for GaN using LDA calculation.
Source: Authors, (2024).

Figure 3: Total energy per molecule as a function of volume for $GaAs_{1-x}N_x$ (x= 0.063) using LDA calculation.
Source: Authors, (2024).
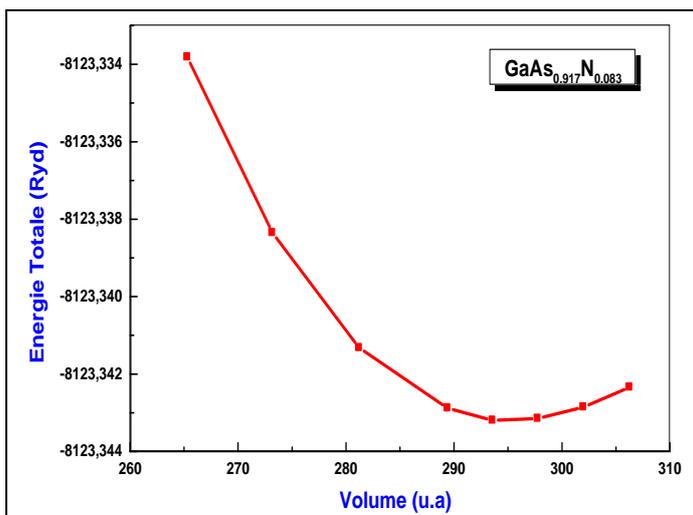
Figure 4: Total energy per molecule as a function of volume for $GaAs_{1-x}N_x$ (x=0.083) using LDA calculation.
Source: Authors, (2024).

Figure 5: Total energy per molecule as a function of volume for $GaAs_{1-x}N_x$ (x=0.125) using LDA calculation.
Source: Authors, (2024).

To determine the equation of state, we fit our DFT total energy calculations, E(V), to the Murnaghan equation of state [43]:

$$E(V) = E_0 + \frac{B}{B(B-1)}\left[V\left(\frac{V_0}{V}\right)^{B_0} - V_0\right] + \frac{B_0}{B_0'}(V - V_0) \qquad (9)$$

where E_0 is the energy at equilibrium volume V_0, B0 is the bulk modulus, and B′ is its pressure derivative. By minimizing the total energy with respect to volume, we obtained the equilibrium lattice constant, bulk modulus, and its derivative for both binary and ternary compounds. These results are summarized in and Table I.

Table 1: The structural parameters of the investigated compounds. V_0 is the equilibrium volume per unit formula ($V_0= a_0^3/4$ for binary, $V_0= (c_0 /a_0)$. $a_0^3/4$ for the tetragonal ternaries), a_0 represents the lattice constant for the binaries and ternaries, B is the bulk modulus and B' is its pressure derivative.

	$V_0(Å^3)$	$a_0 (Å^3)$	c_0/a_0	B (GPa)	B'
x = 0 Exp Theoretical studies	44.989	5.646 5.653[19]· 5.664[41] 5.666[42],	1	68.699 75.50[48] 69.71[41], 69.60[42], 76.47[14]	4.765 4.28 [14]
x = 1 Exp Theoretical studies	22.476	4.480 4.50 [43], [44] [46] 4.46[45] 4.48[48] 4.50[10], 4.56[49], 4.55[47]	1	192.564 190.932[45], 206.9[44] 189.488[10]	4.963 5.30[47] 4.46[10]
x = 0.125	42.600	5.544	2	73.701	4.556
x = 0.083	43.342	5.576	3	71.788	4.798
x = 0..063	43.716	5.592	4	71.935	4.789

Source: a Ref [19], b Ref [14], c Ref [10], d Ref [41], e Ref [42], f Ref [43], g Ref [44] , h Ref [45] , i Ref [48] , k Ref [49].

Our calculated equilibrium lattice parameters for GaN and GaAs are 4.480 Å and 5.646 Å, respectively, exhibiting deviations of only 0.69% and 0.75% from the experimental values of 4.511 Å and 5.6535 Å [14], [50]. The computed bulk modulus for zinc-blende GaAs and GaN is in good agreement with experimental data and previous theoretical studies [14]. Notably, GaN demonstrates a lower compressibility compared to GaAs.
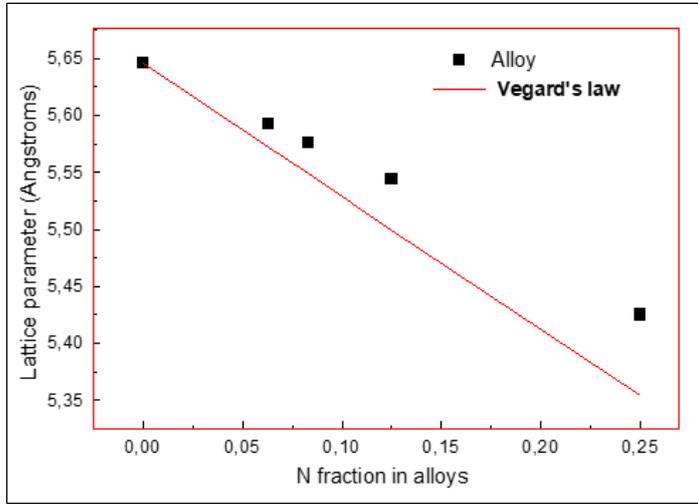
Figure 6: Lattice constant versus nitrogen concentration x in GaAs1-xNx.
Source: Authors, (2024).

For a given nitrogen concentration, the ternary alloys exhibit nearly identical equilibrium lattice parameters, displaying a linear variation (Figure 6).

However, a significant positive deviation from Vegard's law is observed for $GaAs_{1-x}N_x$, with an upward bowing parameter of -0.385 Å determined through polynomial fitting. This deviation is primarily attributed to the substantial size mismatch and lattice constant disparity between GaAs and GaN [33].

The bulk modulus of $GaAs_{1-x}N_x$ deviates notably from a linear concentration dependence, exhibiting a downward bowing of 45.82 GPa. This disparity results in a considerable deviation in rigidity for all systems studied. Notably, an increase in nitrogen concentration within $GaAs_{1-x}N_x$ correlates with a lattice parameter decrease and a bulk modulus increase, consistent with general trends observed in other III-V semiconductors and alloys [14], [51].

We began by calculating the band structures of the binary compounds GaAs and GaN. Both materials exhibited direct band gaps, with the valence band maximum (VBM) and conduction band minimum (CBM) located at the Γ point in the Brillouin zone. A comparison of our calculated bandgaps (0.206 eV for GaAs and 1.916 eV for GaN) with experimental values (1.52 eV for GaAs and 3.20 eV for GaN [14,51,52]) reveals an underestimation. However, given the focus of this study on qualitative trends rather than quantitative accuracy, this discrepancy does not significantly impact our conclusions.

Subsequently, we calculated the band structures for the ternary alloy $GaAs_{1-x}N_x$ and plotted the resulting gap variations (Fig. 7). A critical consideration when studying ternary alloys is the choice of unit cell. The unit cell employed in our calculations is a supercell, not a primitive cell. Consequently, the calculated band gaps may not always correspond to the true fundamental band gaps, which are typically obtained from calculations using primitive cells. This discrepancy arises from the zone folding effect inherent to supercell calculations.

Normally, if one of the binary constituents has an indirect band gap, the supercell of the ternary alloy might exhibit a spurious direct band gap due to zone folding. However, in the present case, both GaAs and GaN possess direct band gaps at the Γ point. Therefore, zone folding is not expected to alter the fundamental gap nature of the ternary alloy.
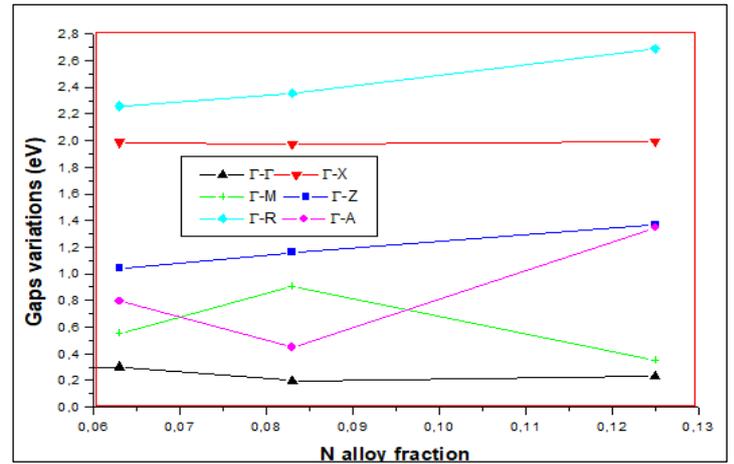
Figure 7: Gaps variation with the N fraction in the alloys.
Source: Authors, (2024).

For selected nitrogen concentrations (x = 0.0625, 0.083, and 0.125) within the dilute nitride regime, our calculations indicate direct band gaps located at the Γ point (Fig. 8, 9 and 10). However, as the nitrogen content increases from $GaAs_{0.937}N_{0.063}$ to $GaAs_{0.875}N_{0.125}$, a nonlinear variation in the Γ-Γ gap is observed. This behavior is similar to that reported for dilute nitride GaAsN alloys. Interestingly, the Γ-M and Γ-A gaps also exhibit nonlinear trends, with the Γ-M gap increasing while the Γ-A gap decreases. This complex behavior is likely attributed to zone folding effects, as the quantum states at these high-symmetry points are linear combinations of states from different high-symmetry points in the reciprocal lattice of the primitive cell.
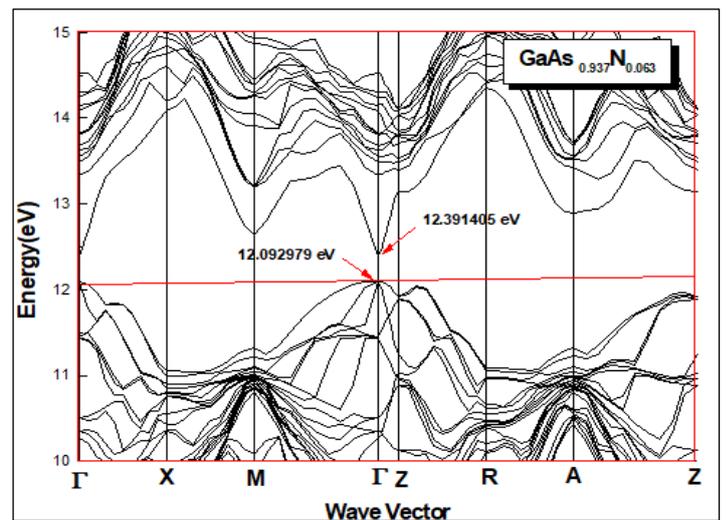
Figure 8: The band structure of the strained bulk $GaAs_{0.937}N_{0.063}$ alloy at a lattice parameter of a(x= 0.063).
Source: Authors, (2024).
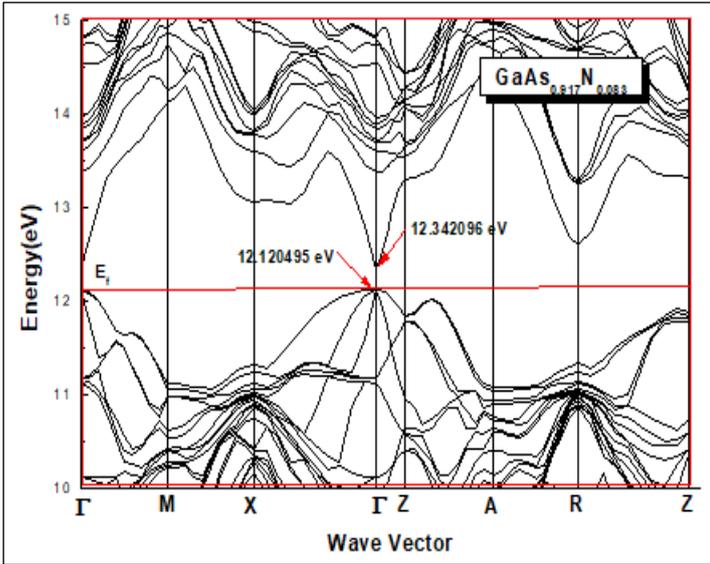
Figure 9: The band structure of the strained bulk $GaAs_{0.917}N_{0.083}$ alloy at a lattice parameter of a(x= 0.0873).
Source: Authors, (2024).
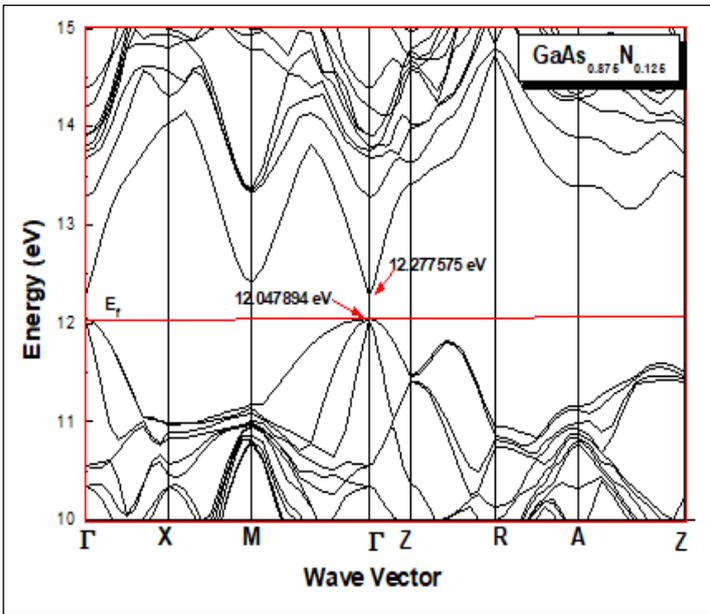
Figure 10: The band structure of the strained bulk $GaAs_{0.875}N_{0.125}$ alloy at a lattice parameter of a(x= 0.125).
Source: Authors, (2024).

The ternary $GaAs_{1-x}N_x$ alloys exhibit a direct bandgap character with both the valence band maximum (VBM) and conduction band minimum (CBM) located at the Γ point in the Brillouin zone. A notable trend is the increase in bandgap energy with increasing nitrogen content (x). However, this variation is nonlinear, indicating a more complex relationship between composition and bandgap than a simple linear interpolation.

Table 2 summarizes the calculated band gaps for the various samples. Our results indicate a strong dependence of the bandgap on nitrogen atom distribution within the supercell, highlighting the significant influence of nitrogen incorporation on the conduction band structure. Even small nitrogen concentrations (a few percent) can dramatically affect the electronic properties of GaAs.

Table 2: The gap energies (in eV) between the upper VB and the lower CB of the zinc blende (ZB) of all the present binary and ternaries.

	x=0	x =1	x= 0.063	x= 0.125	x=0.083
Γ- Γ	0,239	1,916	0.298	0,229	0,221
Γ –X	1,918	4.717	1,987	1,993	1,999
Γ –M	2,642	6.606	0.555	0.354	0.933
Γ –Z	--------	--------	1.043	1.365	1.186
Γ –R	0,828	4.874	2.259	2.688	2.380

Source: Authors, (2024).

Our calculations reveal a pronounced sensitivity of the calculated band gaps to the spatial distribution of nitrogen atoms within the supercell. This observation underscores the critical role of nitrogen incorporation in modifying the conduction band structure. Even a modest nitrogen content of a few percent in GaAs can significantly perturb the electronic properties of the material. This sensitivity arises from the formation of localized electronic states associated with nitrogen atoms, which act as perturbations to the host GaAs lattice. These localized states can introduce new energy levels within the band gap, leading to band gap narrowing and altering the overall electronic structure. Consequently, the precise arrangement of nitrogen atoms within the supercell has a substantial impact on the resulting band gap, highlighting the importance of considering configurational disorder effects in theoretical modeling of these materials.

According to the model proposed by Van Vechten and Bergstresser [29], the electronegativity difference between constituent atoms is a critical factor influencing the degree of disorder within an alloy system, which in turn affects the bandgap. In the case of $GaAs_{1-x}N_x$, the varying electronegativity between Ga, As, and N atoms results in different degrees of disorder for different alloy compositions. This disorder contributes to the nonlinear behavior of the bandgap.

To quantify the impact of disorder on the bandgap, we introduced the total curvature parameter (b) for the Γ-Γ transition. Our calculations summarized in the table 3 yielded values of 12.52 eV, 18.56 eV, and 24.66 eV for $GaAs_{0.875}N_{0.125}$, $GaAs_{0.917}N_{0.083}$, and $GaAs_{0.937}N_{0.063}$, respectively. These values suggest a significant increase in disorder with decreasing nitrogen content.

Another crucial factor affecting the bandgap is volume deformation (VD). Our calculations indicate that the contribution of VD to the total energy gap curvature parameter is substantial, especially for the $GaAs_{0.937}N_{0.063}$ alloy. This implies that the lattice expansion due to the incorporation of larger nitrogen atoms plays a dominant role in modifying the bandgap for this particular composition.

Table 3: Calculated bowing parameters b for $GaAs_{1-x}N_x$ alloys. The contributions due to volume deformation (b_{VD}), electronegativities (b_{CE}), and structural relaxations (b_{SR}) are also listed. All values are in eV.

Composition x	x= 0.125	x=0.083	x=0.063
b_{VD}	14.585	22.609	30.044
b_{CE}	-2.195	-4.210	-5.447
b_{SR}	0.134	0.165	0.061
b	12.525	18.564	24.662

Source: Authors, (2024).

The significant role of volume deformation (VD) in contributing to the band gap bowing parameter is directly linked to the substantial lattice mismatch between the constituent binary compounds GaAs and GaN. In many alloy systems, the VD term is closely correlated with the overall volume of the unit cell, as represented by the lattice parameter (a). Consequently, the pronounced VD bowing parameter observed in $GaAs_{1-x}N_x$ can be attributed to the considerable difference in lattice constants between GaAs and GaN.

It is important to note that while charge exchange (ECB) can also influence bandgap bowing, its contribution is significantly smaller than that of VD in this system. This disparity is consistent with the relatively low ionicity of the constituent elements.

Structural relaxation (bSR), which accounts for atomic displacements from ideal lattice positions, is found to have a minimal impact on bandgap bowing in $GaAs_{1-x}N_x$ due to the limited lattice mismatch between the two binary compounds. This study primarily focused on nitrogen concentrations above 7% (Figure 11). A comprehensive understanding of the bandgap bowing behavior at lower nitrogen levels would require further investigation.
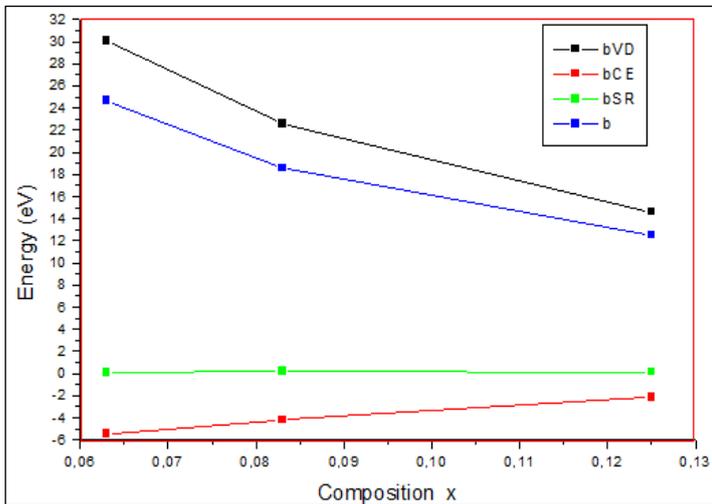
Figure 11: Curvature parameter variation b and the three contributions bVD, bCE, and bSR considering concentration x.
Source: Authors, (2024).

IV. CONCLUSIONS

This study employed ab-initio FPLMTO calculations to investigate the structural properties of cubic and tetragonal Ga(As,N) alloys, focusing on the critical role of interstitial regions, to clarify the mechanism of the large band gap bowing of the dilute nitride semiconductors, we calculated band edge energies of $GaAs_{1-x}N_x$.

Our findings indicate a complex interplay between volume deformation (VD), charge transfer (CE), and structural relaxation (SR) in determining the band gap bowing behavior of these alloys.

For the majority of compositions studied, VD emerges as the dominant factor influencing band gap bowing, with CE playing a comparatively minor role. Structural relaxation effects (SR) were found to be relatively weak in these systems. Collectively, VD and SR, constituting the structural component, primarily govern the overall band gap bowing.

It is important to note that the present investigation focused on nitrogen concentrations exceeding 7%. A comprehensive understanding of band gap bowing across the entire composition range would require further studies.

These results provide valuable insights into the fundamental mechanisms underlying band gap bowing in $GaAs_{1-x}N_x$ alloys, contributing to the development of more accurate theoretical models and facilitating the design of optoelectronic devices based on these materials.

V. AUTHOR'S CONTRIBUTION

Conceptualization: Mimouna Oukli , Ghlam Karima, Seyfeddine Bechekir.
Methodology: Mimouna Oukli , Ghlam Karima, Seyfeddine Bechekir.
Investigation:. Mimouna Oukli , Ghlam Karima, Seyfeddine Bechekir.
Discussion of results: Mimouna Oukli , Ghlam Karima, Seyfeddine Bechekir.
Writing – Original Draft: Mimouna Oukli , Ghlam Karima, Seyfeddine Bechekir.
Writing – Review and Editing: Mimouna Oukli , Ghlam Karima, Seyfeddine Bechekir.
Supervision: Mimouna Oukli , Ghlam Karima, Seyfeddine Bechekir.
Approval of the final text: Mimouna Oukli , Ghlam Karima, Seyfeddine Bechekir.

V. ACKNOWLEDGMENTS

VI. REFERENCES

[1] Paola Prete , Nico Lovergine, Progress in Crystal Growth and Characterization of Materials, Volume 66, Issue 4, November 2020, 100510**,**

[2] Z. Zaaboub , F. Hassen, H. Maaref, Solid State Communications. 314-315 (2020) 113913.

[3] Jian V. Lia, Man Hoi Wongb, Thin Solid Films 758 (2022) 139422. Volume 758, 30 September 2022, 139422.

[4]Takashi Tsukasakia, Naoki Mochidaa , Miki Fujitab , Toshiki Makimotoa, , Physica B: Condensed Matter, Volume 625, 15 January 2022, 413482.

[5] Arpad Kosaa,, Lubica Stuchlikovaa , Ladislav Harmathaa , Jaroslav Kovaca , Beata Scianab ,Wojciech Dawidowskib , Marek Tlaczalab, Materials Science in Semiconductor Processing, Volume 74, February 2018, Pages 313-318,

[6] Justin C. Goodrich, Damir Borovac, Chee-Keong tan & Nelson tansu, Scientific RepoRts | (2019) 9:5128.

[7] Wadi Bachir Bouiadjraa, Abdelkader Saidanea , Abdelkader Mostefaa Mohamed Heninib , M. Shafib ,Superlattices and Microstructures, Volume 71, July 2014, Pages 225-237.

 [8] Takashi Tsukasaki , Naoki Mochida, Miki Fujita , Toshiki Makimoo, Physica B: Condensed Matter, Volume 625, 15 January 2022, 413482.

[9] Francesco Biccari, Alice Boschetti, Giorgio Pettinari, Federico La China, Massimo Gurioli, Francesca Intonti, Anna Vinattieri, MayankShekhar Sharma, Mario Capizzi, Advanced   Material, Volume 30, Issue 21, May 24, 2018,1705450.

[10] S Gagui, H meradji, S Ghemid, Y Megdoud, B ZAIDI, B Ul haq, R Ahmed, B Hadjoudja , B Chouial, Bull. Mater. Sci. (2023) 46:63

[11] S gagui, S Ghemid, H Meradji, B Zaidi, Bakhtiar Ul haq, R Ahmed, B Hadjoudja, B Chouial and S A Tahir, Pramana , J. Phys. (2023) 97:145 .

[12] M. Lahoual, · A. Gueddim , · N. Bouarissa, Transactions on Electrical and Electronic Materials (2019) 20:344–349.

[13] Eßer et al. Appl. Phys. Lett. 107, 062103 (2015).

[14] Yibo Wang, Yan Liu, Genquan Han, Hongjuan Wang, Chunfu Zhang, Jincheng Zhang, Yue Hao, Superlattices and Microstructures, Volume 106, June 2017, Pages 139-146.

[15] I. Vurgaftman, J.R. Meyer, J. Appl. Phys. 94, 3675 (2003).

[16]. A. Gueddim, R. Zerdoum, N. Bouarissa,. J. Phys. Chem. Solids 67(8), 1618–1622 (2004).

[17] K.M. Yu, W. Walukiewicz, J. Wu, J.W. Beeman, J.W. Ager, E.E. Haller, W. Shan, H.P. Xin, C.W. Tu, Synthesis of III–Nx–V1-x thin _lms by N ion implantation. Appl. Phys. Lett. 78, 1077 (2001).

[18] S. Ben Bouzid, F. Bousbih, R. Chtourou, J.C. Harmand, P.Voisin, E_ect of nitrogen in the electronic structure of GaAsN and GaInAs(N) compounds grown by molecular beam epitaxy. Mater. Sci. Eng. B 112, 64 (2004).

[19] F. Hassena, Z. Zaabouba , M. Bouhlela , M. Naffoutia , H. Maarefa , N.M. Garni, Thin Solid Films, Volume 594, Part A, 2 November 2015, Pages 168-171.

[20] X.Z. Chen , D.H. Zhang , Y.J. Jin , J.H. Li , J.H. Teng , N. Yakovlev , Journal of Crystal Growth, 362 (2013) 197–201.

[21] Chuan-Zhen Zhao, Na-Na Li, Tong Wei, Chun-Xiao Tang, Ke-Qing Lu, Appl.Phys. Lett. 100 (2012) 142112.

[22] W. Shan, W. Walukiewicz, J.W. Ager III, E.E. Haller, J.F. Geisz, D.J. Friedman, J.M. Olson, S.R. Kurtz, Phys. Rev. Lett. 82 (1999) 1221.

[23] J. Wu, W. Walukiewicz, K.M. Yu, J.W. Ager III, E.E. Haller, Y.G. Hong, H.P. Xin, C.W. Tu, Phys. Rev. B 65 (2002) 241303.

[24] A. Lindsay, E.P. O'Reilly, Phys. Rev. Lett. 93 (2004) 196402.

[25] E.P. O'Reilly, A. Lindsay, S. Tomic, M. Kamal-Saadi, Semicond. Sci. Technol. 17 (2002) 870.

[26] W.J. Fan, M.F. Li, T.C. Chong, J.B. Xia, J. Appl. Phys. 79 (1996) 188.

[27] L. Bellaiche, S.-H. Wei, A. Zunger, Appl. Phys. Lett. 70 (1997).

[28] L. Bellaiche, S.-H. Wei, A. Zunger, Phys. Rev. B 54 (1996) 17568.

[29] Kurt A. Mader, A. Zunger, Phys. Rev. B 50 (1994) 17393.

[30] P.R.C. Kent, A. Zunger, Phys. Rev. B 64 (2001) 115208.

[31] V. Timoshevskii, M. Côté, G. Gilbert, R. Leonelli, S. Turcotte, J.-N. Beaudry, P. Desjardins, S. Larouche, L. Martinu, R.A. Masut, Phys. Rev. B 74 (2006) 165120.

[32] C.-K. Tan, J. Zhang, X.-H. Li, G. Liu, B.O. Tayo, N. Tansu, J. Display Technol. 9 (2013) 272L.

[33] S. T. Murphy, A. Chroneos, C. Jiang, U. Schwingenschlögl, R. W. Grimes, PHYSICAL REVIEW B 82, 073201 2010.
[34] M. Ferhat, Phys. Status Solidi b 241 (2004) R38.

[35] S.Y.Savrasov, Phys Rev B 54, 16470 (1996).

[36] S.Y.Savrasov, Phys Rev B 54, 16470 (1996).

[37] http://www.physics.ucdavis.edu/~mindlab/

[38]http://www.fkf.mpg.de/andersen/

[39] P. Hohenberg, W. Kohn, Phys. Rev. 136, B864 (1964).

[40] Perdew J P and Wang Y Phys. Rev. B 45, 13244 (1992).

[41] J.E. Bernard, A. Zunger, Phys. Rev. B 36 (1987) 3199.

[42] M. Ferhat, F. Bechstedt, Phys. Rev. B 65 (2002) 075213.

[43] F.D.Murnaghan, Proc. Natl. Acad. Sci. USA. 30, 5390 (1944).

[44] M.J. Espitia R et al. / Journal of Magnetism and Magnetic Materials 451 (2018) 295–299.

[45] L.I. Karaouzène et al. / Optik 168 (2018) 287–295

[46] M. Issam Ziane, et al., Mater. Sci. Semicond. Process. 16 (2013) 1138,

[47] M. Abu-Jafar, A.I. Al-Sharif, A. Qteish, Solid State Commun. 116 (2000) 389,

[48] S. Adachi, J. Appl. Phys. 61 (1987) 4869.

[49] H. Baaziz, Z. Charifi, A.H. Reshak, B. Hamad, Y. Al-Douri, Appl. Phys. A 106 (2012) 687.

[50] High-pressure band parameters for GaAs: first principles calculations S. Saib , N. Bouarissa b, Solid-State Electronics 50 (2006) 763–768

[51] K. Beladjal,A. Kadri,K. Zitouni,K. Mimouni - Superlattices and Microstructures, Vol. 155, (2021), pp 106901.

[52] M. Briki et al. / Superlattices and Microstructures 45 (2009) 80_90